Applied Surface Science 399 (2017) 663–669

Contents lists available at ScienceDirect

Applied Surface Science

journal homepage: www.elsevier.com/locate/apsusc

Full Length Article

Ferrofluids based on Co-Fe-Si-B amorphous nanoparticles

Tianqi Wang, Xiufang Bian*, Chuncheng Yang, Shuchun Zhao, Mengchun Yu

Key Laboratory for Liquid-Solid Structural Evolution and Processing of Materials, Ministry of Education, Shandong University, Jinan 250061, China

ARTICLE INFO

Article history:
Received 5 September 2016
Received in revised form
13 December 2016
Accepted 18 December 2016
Available online 19 December 2016

Keywords:
Ferrofluids
Amorphous nanoparticles
Magnetic property
Stability
Viscosity

ABSTRACT

Magnetic Co-Fe-Si-B amorphous nanoparticles were successfully synthesized by chemical reduction method. ICP, XRD, DSC, and TEM were used to investigate the composition, structure and morphology of Co-Fe-Si-B samples. The results show that the Co-Fe-Si-B samples are amorphous, which consist of nearly spherical nanoparticles with an average particle size about 23 nm. VSM results manifest that the saturation magnetization (Ms) of Co-Fe-Si-B samples ranges from 46.37 to 62.89 emu/g. Two kinds of ferrofluids (FFs) were prepared by dispersing Co-Fe-Si-B amorphous nanoparticles and $CoFe_2O_4$ nanoparticles in kerosene and silicone oil, respectively. The magnetic properties, stability and viscosity of the FFs were investigated. The FFs with Co-Fe-Si-B samples have a higher Ms and lower coercivity (Hc) than FFs with $CoFe_2O_4$ sample. Under magnetic field, the silicone oil-based FFs exhibit high stability. The viscosity of FFs under different applied magnetic fields was measured by a rotational viscometer, indicating that FFs with Co-Fe-Si-B particles present relative strong response to an external magnetic field. The metal-boride amorphous alloy nanoparticles have potential applications in the preparation of magnetic fluids with good stability and good magnetoviscous properties.

1. Introduction

Magnetic fluids are stable colloidal dispersions of magnetic particles dispersed in a carrier liquid with both fluidity and magnetism. Common magnetic fluids include ferrofluids (FFs) and magnetorheological (MR) fluids. In FFs the nanoparticles are single-domain ones and possess the intrinsic magnetic moments. In MR fluids the particles are magnetically multidomain, and the particle magnetic moment is induced by an external magnetic field [1,2]. Under the effect of external magnetic field, their physical properties can be changed significantly, which have been exploited in various fields such as brake [3], sensor [4], sealing [5], lubricating [6], target drug delivery [7], removal of water pollutants [8], and so forth.

To date, the most commonly used particles in magnetic fluids are ferrite prepared by chemical co-precipitation method, including Fe_3O_4 [9,10], $ZnFe_2O_4$ [11],and $CoFe_2O_4$ [12], etc., on account of their good properties of easy manufacture and biocompatibility. However, their also possess low magnetic energy density and low saturation magnetization, which limit their application in high power fields [10,13]. Recent studies manifest that amorphous soft magnetic alloys have great potential applications in the preparation of magnetic fluids due to their unique physical and chemical properties [14]. For example, $Fe_{73.5}Nb_3Cu_1Si_{13.5}B_9$ [13] and $Fe_{78}Si_9B_{13}$ [15] amorphous alloy particles were applied in the preparation of MR fluids and exhibit higher saturation magnetization in comparison with ferrite. Nevertheless, owing to the limitation of the preparation technologies (ball-milling and spraying method), the particles employed in the liquids are difficult to reach the nanometer magnitude, and the oversized particles are especially prone to causing the problems of agglomeration and sedimentation. Beyond that, some amorphous alloys cannot be prepared by these methods due to their high melting points [16]. Chemical reduction, by contrast, is a relatively simple method preparing amorphous alloy nanoparticles [17]. In this method, different metal salts are reduced by reductants such as BH_4^- and $H_2PO_2^-$ usually in an aqueous medium, and a great range of binary and ternary M-B/P (M = Fe, Co, Ni) amorphous magnetic nanoparticles or nanochains [18] can be finally prepared by precisely controlling the reaction conditions. The M-B amorphous alloy nanoparticles obtained, especially in those with the particle size of less than 50 nm, could be good candidates for the preparation of magnetic fluids for their combined properties of the amorphous structures, the size effects of the nanostructures and the good magnetic properties. However, little attention has been paid to the application of metal-boride amorphous alloy nanoparticles into magnetic fluids.

Co-Fe-Si-B amorphous alloys have extensive application in sensors and magnetic recording materials owing to its great soft

* Corresponding author.
E-mail address: xfbian@sdu.edu.cn (X. Bian).

http://dx.doi.org/10.1016/j.apsusc.2016.12.145
0169-4332/

magnetic properties, high glass forming ability (GFA) and giant magnetoimpedance effect (GMI) [19,20]. MR fluids containing Co-Fe-Si-B amorphous microparticles obtained by ball-milling process have also been reported [14]. As mentioned above, the preparation method and the oversized particles limit their further application. Therefore, it is of great interest to explore the possibility of preparing Co-Fe-Si-B alloy by chemical reduction method.

In this work, we firstly report the synthesis and applications in FFs of Co-Fe-Si-B amorphous nanoparticles made by a chemical reduction method. The structure, composition and magnetic properties of the Co-Fe-Si-B amorphous nanoparticles and the magnetic properties, stability and viscosity of the corresponding FFs were investigated. In comparison with $CoFe_2O_4$ based FFs, the Co-Fe-Si-B based FFs exhibit better soft magnetism and respond stronger to an external magnetic field.

2. Experimental

2.1. Materials

Cobalt chloride ($CoCl_2{\cdot}6H_2O$), ferric chloride ($FeCl_3{\cdot}6H_2O$), ferrous chloride ($FeCl_2{\cdot}4H_2O$), sodium hydroxide (NaOH), sodium fluosilicate (Na_2SiF_6), sodium borohydride ($NaBH_4$), Silicon oil, kerosene, sodium oleate, absolute ethyl alcohol and acetone were all purchased from Sinopharm Chemical Reagent Co. Ltd (Shanghai, China). All the starting chemicals used were of analytical reagent (AR) grade without further purification. Deionized water was used in this experiment.

2.2. Synthesis of $CoFe_2O_4$ and Co-Fe-Si-B nanoparticles

The $CoFe_2O_4$ nanoparticles were prepared by chemical co-precipitation method [12]. The ion reaction equation is described as follows:

$$Co^{2+}+2Fe^{3+}+8OH^{-}=CoFe_2O_4+4H_2O.$$

A right amount of NaOH solution was added to a mixed solution in which the molar ratio of Co^{2+} and Fe^{3+} was 1:2. Then the mixture solution was stirred in beaker at 373 K for 2 h. The black $CoFe_2O_4$ nanoparticles were obtained after deionized water's washing and ultrasonic cleaning.

The Co-Fe-Si-B nanoparticles were prepared by chemical reduction. In the synthesis process, certain amount of $CoCl_2{\cdot}6H_2O$, $FeCl_2{\cdot}4H_2O$ and Na_2SiF_6 were dissolved in 200 ml of 50% ethanol solution (v/v) with magnetic stirring. Then, 50 ml of 0.8 M $NaBH_4$ aqueous solution was added dropwise into above solution at a speed of 1.5 ml/min at 20 °C with mechanical stirring and supersonic dispersion. The NaOH solution was used to adjust the pH of $NaBH_4$ aqueous solution to 12–13. After stirring for 2 h, the black precipitate was separated using a magnet. The solid was rinsed with deionized water and acetone for several times, then stored in absolute ethyl alcohol for further use. The molar ratio of $[SiF_6]^{2-}$ was changed in the mixed solution for comparison and the preparation conditions are listed in Table 1.

2.3. Sodium oleate modification of nanoparticles and synthesis of ferrofluids

The nanoparticles obtained were dispersed in 200 ml of deionized water. Then, 0.1 g sodium oleate were added to the suspension, stirred for 3 h at 30 °C, and then cleaned repeatedly by acetone. After that, the precipitate was dried in vacuum for 12 h at 45 °C. The modified nanoparticles were dispersed in 50 ml of kerosene and silicone oil separately. After 2 h' stirring the stable ferrofluids containing 4.0 vol% of magnetic particles were obtained.

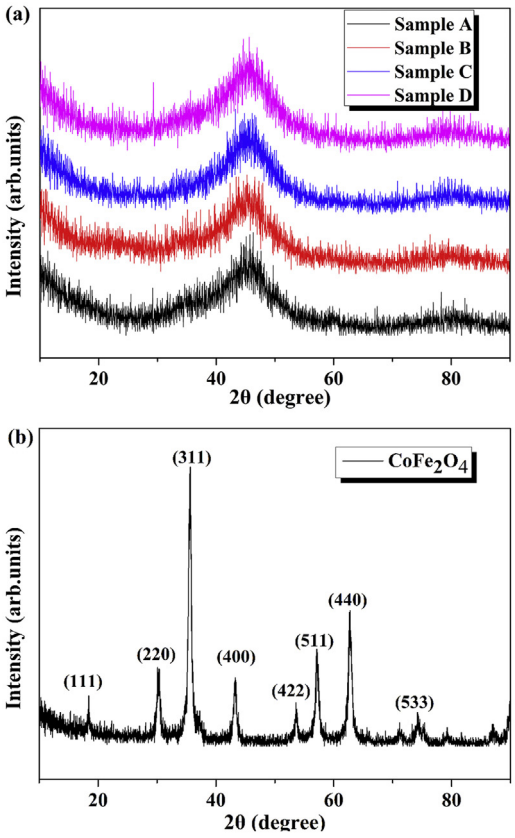

Fig. 1. The XRD patterns of (a) Co-Fe-Si-B nanoparticles for samples A, B, C and D and (b) $CoFe_2O_4$ nanoparticles.

2.4. Characterization

The precise compositions of the four samples were analyzed by inductively coupled plasma atomic emission spectrometry (ICP-AES, Perkin Elmer 7300DV). The structure of the four samples and $CoFe_2O_4$ nanoparticles were examined by X-ray diffraction (XRD; Rigaku D/MAX-2500/PC) with Cu Ka radiation, selective area electronic diffraction (SAED; JAPAN, JEOL, JEM-2100F), and differential scanning calorimeter (DSC; NETZSCH, DSC 404) at a heating rate of 20 °C/min. The morphology and size of the four samples were identified by scanning electron microscope (SEM; Germany, ZEISS, SUPRA55) coupled with Energy Dispersive X-ray Detector (EDX) and transmission electron microscopy (TEM; JAPAN, JEOL, JEM-2100F). The hysteresis loops of the samples and ferrofluids were measured by a vibrating sample magnetometer (VSM; U.S. LDJ, LS7307-9309) in the applied magnetic field up to 8 kOe at room temperature. The magnetic weight was investigated by Gouy magnetic balance (GMB; Shanghai, China, FD-TX-FM-A) under an applied magnetic field of 100 mT at room temperature. The viscosity of FFs under different applied magnetic fields was carried out by a rotational viscometer (Theta industries, Inc. U.S. DV-III) coupled with permanent magnet.

3. Results and discussion

Fig. 1 shows the XRD patterns of Co-Fe-Si-B particles for four samples and $CoFe_2O_4$ particles. As shown in Fig. 1(a), four kinds of Co-Fe-Si-B particles consist of a single broad peak in the 2θ range of 40°∼50°, and no crystalline peak can be seen, which indicates that four kinds of Co-Fe-Si-B particles obtained above, have a typical amorphous structure. The characteristic peaks shown in Fig. 1(b) for (111), (220), (311), (400), (422), (511) and (440) crystal planes

Table 1
Preparation conditions and compositions of Co-Fe-Si-B particles.

Samples	Concentration of the mixed solution (mol/L)			$(Co^{2+}+Fe^{2+})/[SiF_6]^{2-}$ ratio in the mixed solution	Alloy compositions (at.%)			
	Co^{2+}	Fe^{2+}	$[SiF_6]^{2-}$		Co	Fe	Si	B
A	0.04	0.007	0.0067	7	55.54	9.89	3.37	31.20
B	0.04	0.007	0.0078	6	55.48	10.15	5.28	29.09
C	0.04	0.007	0.0093	5	57.75	10.55	5.79	25.91
D	0.04	0.007	0.0117	4	52.17	9.19	12.50	26.14

coincide with the standard $CoFe_2O_4$ XRD spectrum, indicating the cubic spinel structure of the $CoFe_2O_4$ particles.

The DSC curves of as-prepared Co-Fe-Si-B particles for four samples with a heating rate of 20 °C/min are shown in Fig. 2. Sample C and D exhibit similar curves with only one exothermic peak at 484 °C and 486 °C respectively, indicating a single stage crystallization process. Sample A and B exhibit two exothermic peaks demonstrating two stages crystallization process, which may be connected with two different amorphous phases [21]. And exothermic peaks in Sample B are overlapped, indicating a complex crystallization process [22]. The DSC results further confirm that all four samples are amorphous.

The compositions of Co-Fe-Si-B particles are determined by ICP-AES. The results show that the Si element was successfully reduced by this method. The total concentration of the Co, Fe, Si and B accounts for about 80% of the whole, and the rest is O element, which is mainly due to the oxidation during the reaction process according to similar studies by other authors [23,24]. For simplicity's sake, we neglected the impurity in the samples and normalized the composition to 100%. The normalized results are listed in Table 1. It can be seen that the composition of Si increases with concentration of the $[SiF_6]^{2-}$ increasing. The B content in as-prepared samples is within the range of 25.91% to 31.20%. The mole ratio of Co/Fe is slightly lower than the Co^{2+}/Fe^{2+} in the mixed solution, meaning that most of the metal ions were reduced by $NaBH_4$.

TEM image of sample B (Fig. 3a) demonstrates that the sample is composed of nearly spherical particles. As shown in Fig. 3c, the mean diameter of the particles is about 23 nm, which was estimated by measuring about 200 particles. According to similar reports in recent decades on the magnetic structure of the chemical reduced magnetic nanoparticles, we speculate that the sizes of the Co-Fe-Si-B nanoparticles we obtained are close to the size of single-domain

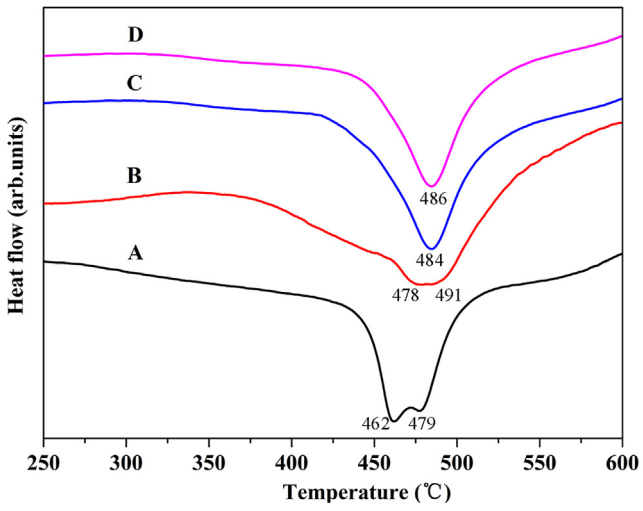

Fig. 2. DSC curves of as-prepared Co-Fe-Si-B particles for samples A, B, C and D with a heating rate of 20 °C/min.

[25–27]. Agglomeration can be observed as a result of the high surface energy of amorphous nanoparticles [28]. The corresponding SAED image displays only a diffraction halo rather than distinct dots or rings, indicating the amorphous structure of the sample, which is in accordance with the XRD and DSC results mentioned above. Fig. 3b and d shows that $CoFe_2O_4$ nanoparticles are regular spheres with an average diameter of about 9 nm. The composition of sample B was also investigated by EDX analysis, the results showed that the composition of the sample B can be expressed as $Co_{55.49}Fe_{9.97}Si_{5.57}B_{28.97}$. The measurement error of EDX analysis was less than 2%, and the EDX result is well in coincident with the ICP results above.

The magnetic properties of as-prepared Co-Fe-Si-B particles and $CoFe_2O_4$ particles are shown in Fig. 4, the inset are enlarged views of the hysteresis loops at low magnetic fields. It can be seen that the hysteresis loops of all four kinds of Co-Fe-Si-B particles are narrower than that of the $CoFe_2O_4$ particles. The magnetic parameters of different nanoparticles are summarized in Table 2. The saturation magnetization (Ms) of the $CoFe_2O_4$ particles is only 31.11 emu/g in our research, while the Ms of Co-Fe-Si-B particles is larger, increasing from 49.11 to 62.89 emu/g, and then dropping rapidly to 46.37 emu/g. The different Ms values of Co-Fe-Si-B particles can be explained by the different compositions [21,29] based on the ICP results above. Sample C exhibits the highest Ms value among the four samples, which is attributed to the highest Co and Fe content and the lowest B content. The high coercivity (Hc) of $CoFe_2O_4$ particles is due to the high structure anisotropy [30], while the Hc of Co-Fe-Si-B particles is significantly lower than $CoFe_2O_4$ particles owing to the disordered structure. Among all four samples, samples B and D have relatively lower Hc (116 Oe and 127 Oe respectively). The above results indicate that the small change of Si content have a significant effect on the magnetic properties of the Co-Fe-Si-B particles. Co-Fe-Si-B particles show semi-hard magnetic character. Here, we selected samples B, which possess the relative good soft magnetism, to prepare magnetic fluids.

As mentioned above, the physical properties of magnetic fluids can be changed significantly under the effect of external magnetic field, so it is important to investigate the response of magnetic fluids to an external magnetic field. The most commonly used method is to measure the magnetization curve $M(H)$ [31,32]. In dilute systems, the FFs can be well described by the one-particle model [33], in which the particles are treated as an ideal paramagnetic gas. By applying the Langevin function $L(\alpha) = \coth(\alpha) - 1/\alpha$, the equilibrium magnetization can be written. Nevertheless, in concentrated FFs, experiments results and computer simulations show an essential deviation from the Langevin function, which is mainly due to the interactions between the particles [34,35]. And there are many theoretical models to evaluate the magnetic properties by taking account of the dipole–dipole interactions [36], for example, the mean-field model [37] and the mean-spherical model [38] for FFs with low or moderate volume concentrations, and the second-order thermodynamic perturbation model [39] for dense FFs.

Fig. 5 shows magnetization curves of different FFs with the same volume fraction $\varphi = 4.0\%$: silicone oil-based FFs and kerosene-based FFs with sample B and $CoFe_2O_4$ particles. The results show that the

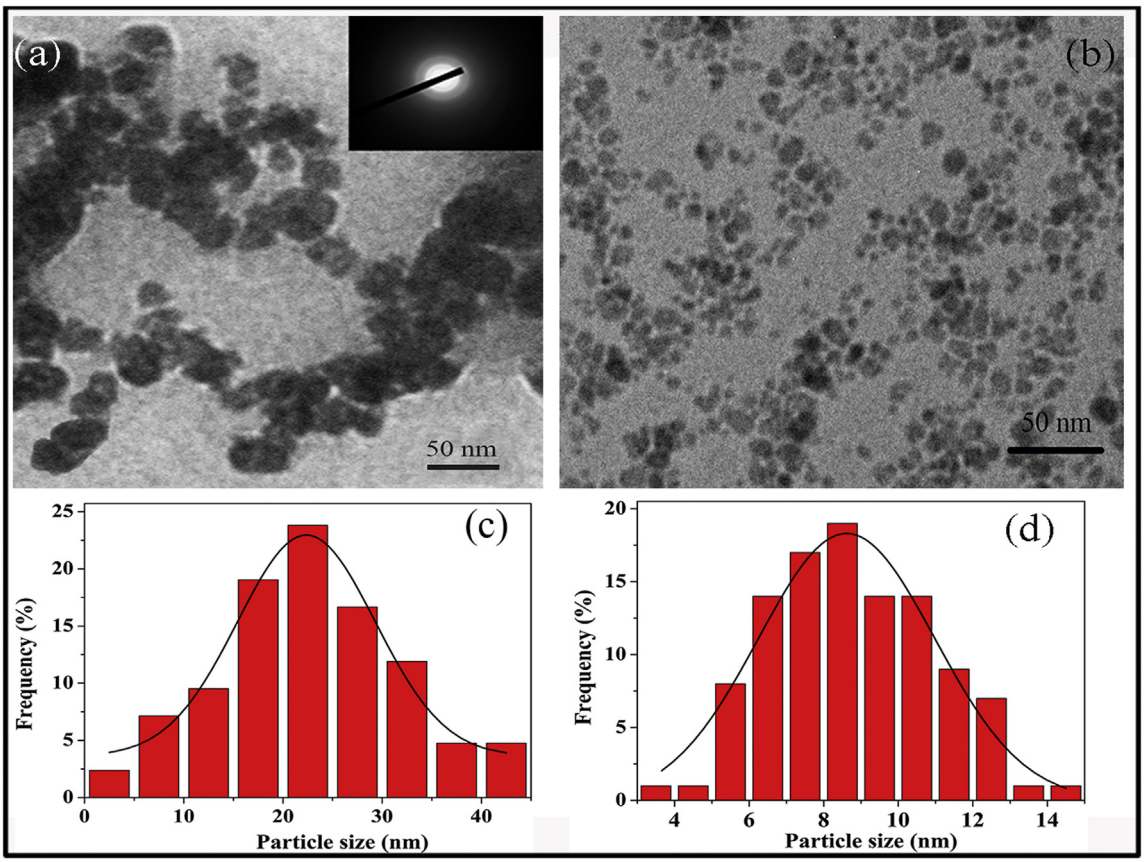

Fig. 3. (a) TEM image and the corresponding SAED image of sample B; (b) TEM image of $CoFe_2O_4$ particles; (c) Particle size distribution of sample B, and (d) Particle size distribution of $CoFe_2O_4$ particles.

Ms of kerosene-based FFs is slightly higher than that of silicone oil-based FFs, which may be due to the diffenent density of the two carrier. The silicone oil-based FFs with sample B have the highest Ms value (1.79 emu/g), which is higher than that of silicone oil-based FFs with $CoFe_2O_4$ particles (0.62 emu/g). This demonstates that the newly synthesized ferrofluids show greater magnetic response.

Stability is an important characteristic for magnetic fluids. As mentioned above, agglomeration and sedimentation, which occur owing to strong dipole–dipole attraction between magnetic particles and great density mismatch between particles and carrier liquid, limit wide use of magnetic fluids [40,41]. Herein, we use sodium oleate as surfactant. The stability of four kinds of FFs was investigated by GMB under a magnetic field of 100 mT. As shown in Fig. 6, the magnetic weight of all four FFs drop quickly at the very start, then change to stabilize in a few hours. FFs with samples B exhibit higher initial magnetic weight than FFs with $CoFe_2O_4$, which is due to the higher Ms value of samples B. The total changing trend of silicone oil-based FFs is relatively smooth than kerosene-based FFs, which indicate that silicone oil-based FFs are more stable. This can be explained that silicone oil possess higher density than kerosene, which is conducive to reduce the density difference between carrier liquids and particles [41].

The magnetoviscous properties of magnetic fluids have also drawn considerable interests in both academic and industrial areas [40]. In this work, a rotational viscometer coupled with permanent magnet (Fig. 7) was used to investigate the variation of viscosity of silicone oil-based FFs with temperature and magnetic field.

Fig. 8 shows viscosity versus temperature curves of silicone oil-based FFs under different magnetic fields and viscosity versus magnetic field strength curves at different temperatures. The results show that the viscosity of the FFs decrease with the temperature increase, which is similar to the previous reports [42,43]. The influence of temperature on the viscosity mainly results from the viscosity-temperature characteristics of the carrier liquids (silicone oil). In the absence of magnetic field, FFs have a low viscosity, while the viscosity increases many times when a magnetic field was applied.

The increase in viscosity of FFs under a magnetic field can be explained by the chain formation conception [44]: the nanoparticles in the FFs can form chain-like structures along the direction of

Table 2
Magnetic parameters of different nanoparticles.

Samples	Saturation magnetization (emu/g)		Coercivity (Oe)		Remanent magnetization (emu/g)	
	Negative	Positive	Negative	Positive	Negative	Positive
Samples A	−49.34	49.11	−282	265	−16.34	16.35
Samples B	−52.42	52.77	−117	116	−7.91	7.90
Samples C	−62.89	62.89	−262	252	−0.75	0.55
Samples D	−46.36	46.37	−230	127	−7.93	7.92
$CoFe_2O_4$	−30.99	31.11	−523	521	−16.10	16.06

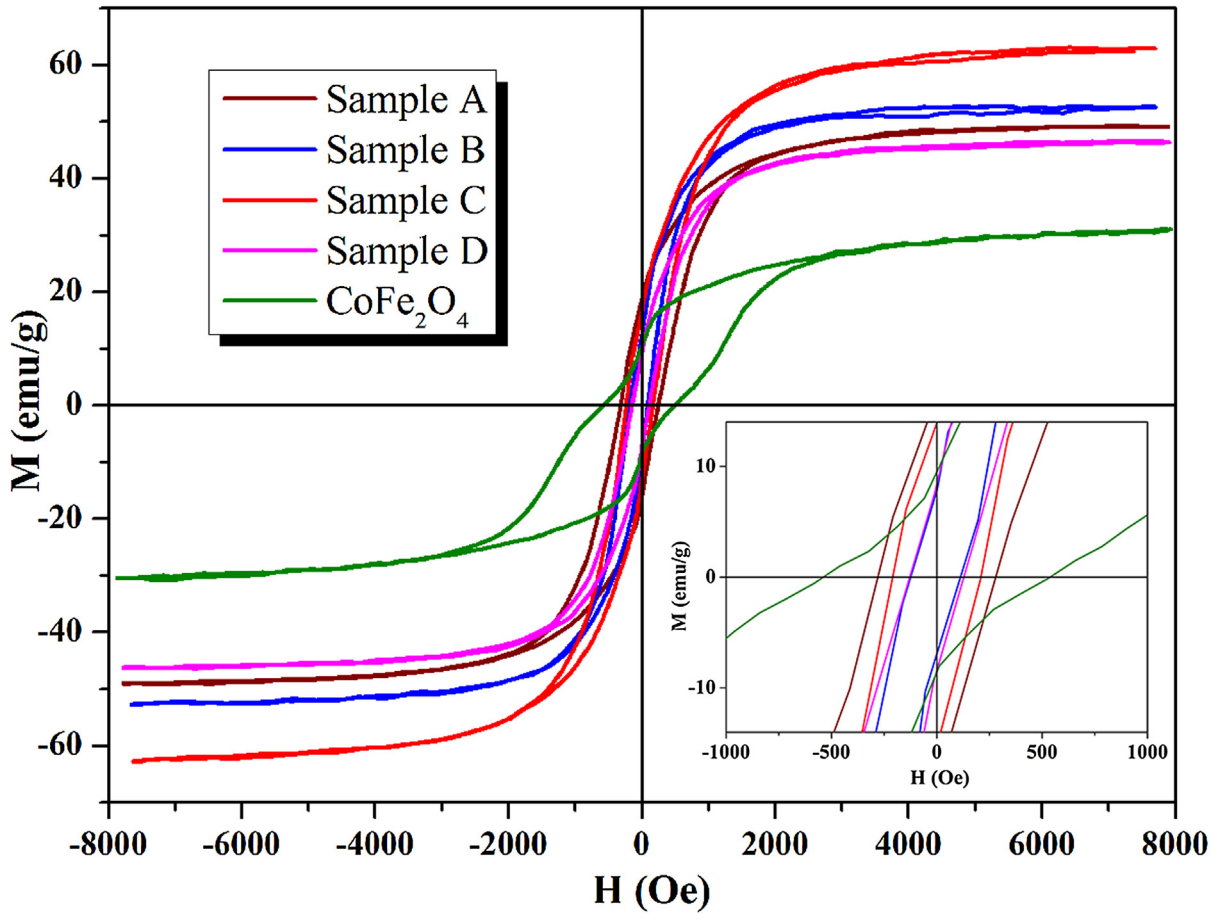

Fig. 4. Hysteresis loops of as-prepared Co-Fe-Si-B particles and $CoFe_2O_4$ particles; the inset are enlarged views of the hysteresis loops at low magnetic fields..

applied magnetic field, and the flow of the liquid is thus hindered by the chain-like structures, causing an increase in viscosity of the FFs. However, the chain formation is observed only in the dipolar systems with rather intensive dipolar interaction [34]. To evaluate the possibility of chain formation, the dipole–dipole interaction parameter λ is usually used,

$$\lambda = \frac{\mu_0 \mathrm{m}^2}{4\pi k_B T \sigma^3} \quad (1)$$

in which μ_0 is the vacuum permeability, $m = \pi M_s x^3/6$ is the particle's magnetic moment (in which M_s is the bulk saturation magnetization of the core material, x is the magnetic core diameter), k_B is the Boltzmann constant, T is the absolute temperature, and σ is the effective particle diameter considering the surface nonmagnetic and sterical layers. The parameter λ expresses the relationship between the interaction energy m^2/d^3 and the thermal energy k_BT of two dipole at close contact [31,34]. The value of λ is less than 1 for ideal FFs containing ferrite with the size

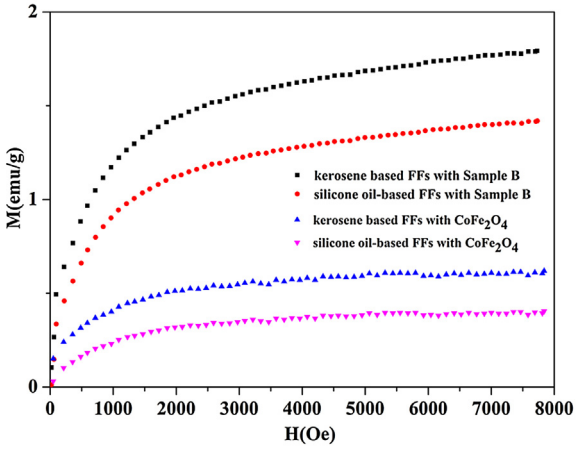

Fig. 5. Magnetization curves of different FFs with the same volume fraction φ = 4.0%: kerosene-based ferrofluids with Sample B and $CoFe_2O_4$ particles, and silicone oil-based ferrofluids with Sample B and $CoFe_2O_4$ particles.

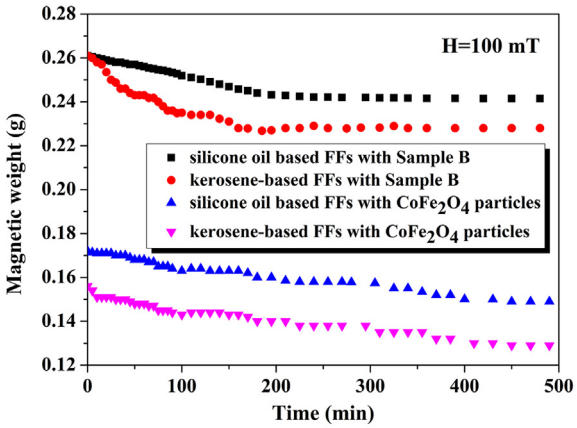

Fig. 6. Magnetic weight versus time curves of silicone-based ferrofluids and kerosene-based ferrofluids with Sample B and $CoFe_2O_4$ particles under a magnetic field of 100 mT.

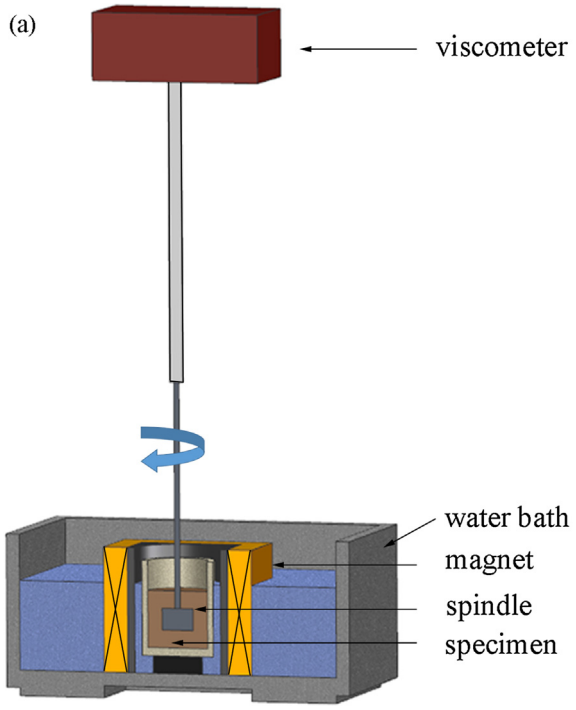

Fig. 7. Schematic of the rotational viscometer coupled with permanent magnet.

~10 nm, in which system the Brownian motion dominates, exhibiting no chainlike structures. When the interaction energy between nanoparticles exceeds the thermal energy, that is, $\lambda > 1$, chainlike structures are formed. For example, in polydisperse systems, the presence of big particles (15–20 nm) above the critical diameter can lead to the larger values of m and λ (3–5). Similarly, in MR fluids, the much larger particles can reach larger values, making it easy to form chainlike structures [15,36].

And in our research, the mean diameter of the Co-Fe-Si-B nanoparticles (23 nm) is close to the limit of single-domain breaking. However, few reports are studied on FFs containing particles in this size, since the big particles in common polydispersed FFs are usually less than 20 nm. The only work was in ref [2],which they presented FFs with spherical CoNi particles of 24 nm in mean diameter and fiberlike CoNi particles of 56 nm in length and 6.6 nm in width, and they observed the induced structures upon the external magnetic field. Although more experiment data are needed, we can speculate the value of λ qualitatively by the equation (1). Here, the M_s is about 3.17×10^5 A/m (the M_s of sample B is about 52.8 emu/g, the density $\rho \approx 6.0\,g/cm^{-3}$), $\sigma \approx x \approx 23$ nm, $\mu_0 = 4\pi \times 10^{-7}\,J\,A^{-2}\,m^{-1}$. The final result is that $\lambda \approx 8.2$. According to experimental and theoretical results by Ivanov et al. [36], the formation of chains starts at a large dipolar coupling $\lambda \geq 3$. So in our experiment, we think that the increase in viscosity of FFs under a magnetic field can be explained by the chain formation conception.

It can also be seen that the viscosity of FFs with Co-Fe-Si-B particles is several times higher than that of FFs with $CoFe_2O_4$ particles when magnetic field strength are equal. What's more, as shown in Fig. 8c, with the magnetic field strength increase, the viscosity of FFs with Co-Fe-Si-B particles increase significantly with about 3.94 cp per Gs of the average change rate, which is more than twice higher than that of FFs with $CoFe_2O_4$ particles. The results indicate that FFs with Co-Fe-Si-B particles present relative strong response to an external magnetic field. The main reason is that Co-Fe-Si-B particles exhibit relative high λ value, which tends to form a stronger dipolar interaction and longer chain-like structures.

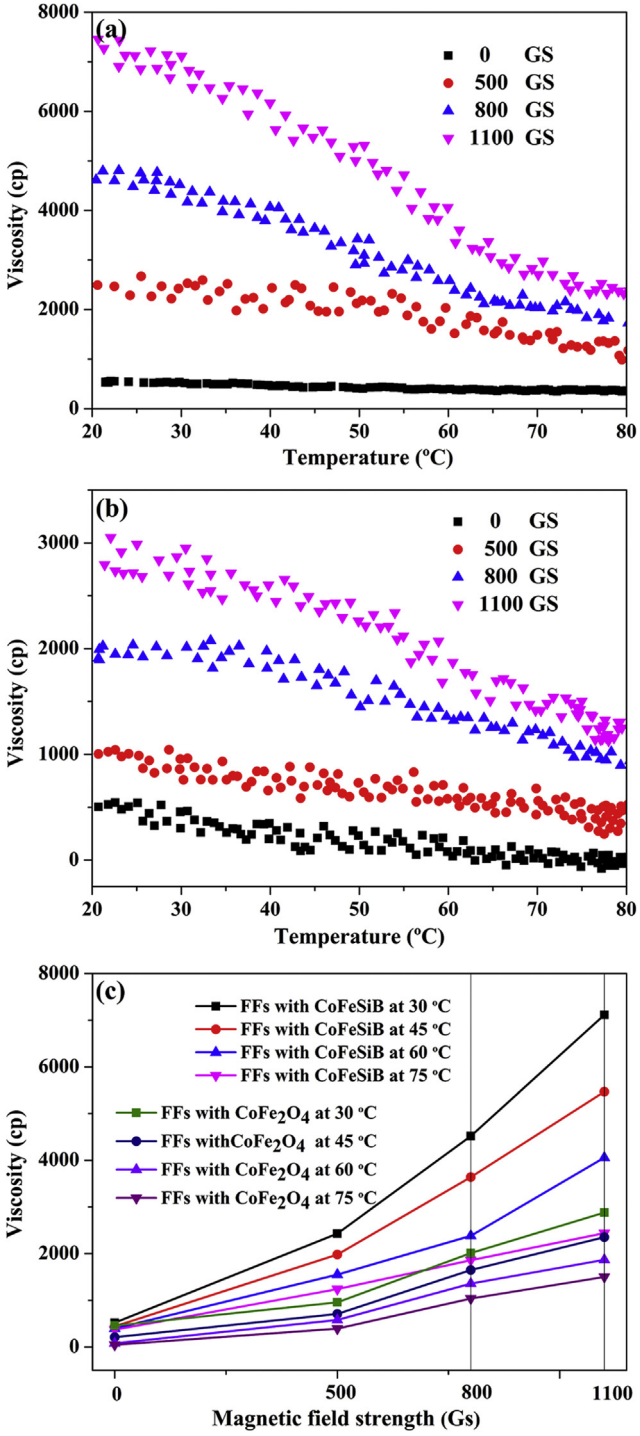

Fig. 8. Viscosity versus temperature curves of silicone oil-based FFs (a) with Co-Fe-Si-B particles and (b) with $CoFe_2O_4$ particles under constant magnetic fields of 0 Gs, 500 Gs, 800 Gs and 1100 Gs, and (c) viscosity versus magnetic field strength curves at 30 °C, 45 °C, 60 °C and 75 °C.

4. Conclusion

This paper firstly reports the synthesis and applications in ferrofluids of Co-Fe-Si-B amorphous nanoparticles by a chemical reduction method. The Co-Fe-Si-B samples are amorphous consisting of nearly spherical particles with an average particle size about 23 nm. The Ms of Co-Fe-Si-B samples range from 46.37 to 62.89 emu/g, which is higher than that of $CoFe_2O_4$ sample, and FFs with Co-Fe-Si-B samples have a higher Ms and lower Hc than FFs with

$CoFe_2O_4$ sample. The results of GMB experiments reveal that the silicone oil-based FFs exhibit high stability under magnetic field. The viscosity of FFs under different applied magnetic fields was also measured and the results indicate that FFs with Co-Fe-Si-B particles present relative strong response to an external magnetic field. The metal-boride amorphous alloy nanoparticles are good candidates for the preparation of magnetic fluids with good stability and good magnetoviscous properties.

Acknowledgement

The authors are grateful for the financial support from the National Natural Science Foundational of China (Grant no. 51571130).

References

[1] A. Joseph, S. Mathew, Ferrofluids: synthetic strategies, stabilization, physicochemical features, characterization, and applications, Chempluschem 79 (2014) 1382–1420.
[2] M.T. Lopez-Lopez, A. Gomez-Ramirez, L. Rodriguez-Arco, J.D. Duran, L. Iskakova, A. Zubarev, Colloids on the frontier of ferrofluids. Rheological properties, Langmuir 28 (2012) 6232–6245.
[3] D.M. Wang, Y.F. Hou, Z.Z. Tian, A novel high-torque magnetorheological brake with a water cooling method for heat dissipation, Smart Mater. Struct. 22 (2013) 025019.
[4] P. Zu, C.C. Chan, T.X. Gong, Y.X. Jin, W.C. Wong, X.Y. Dong, Magneto-optical fiber sensor based on bandgap effect of photonic crystal fiber infiltrated with magnetic fluid, Appl. Phys. Lett. 101 (2012) 241118.
[5] G. Schinteie, P. Palade, L. Vekas, N. Iacob, C. Bartha, V. Kuncser, Volume fraction dependent magnetic behaviour of ferrofluids for rotating seal applications, J Phys D Appl Phys 46 (2013) 395501.
[6] J.R. Lin, R.F. Lu, M.C. Lin, P.Y. Wang, Squeeze film characteristics of parallel circular disks lubricated by ferrofluids with non-Newtonian couple stresses, Tribol. Int. 61 (2013) 56–61.
[7] J.K. Oh, J.M. Park, Iron oxide-based superparamagnetic polymeric nanomaterials: design, preparation, and biomedical application, Prog. Polym. Sci. 36 (2011) 168–189.
[8] N. Ferroudj, J. Nzimoto, A. Davidson, D. Talbot, E. Briot, V. Dupuis, A. Bee, M.S. Medjram, S. Abramson, Maghemite nanoparticles and maghemite/silica nanocomposite microspheres as magnetic Fenton catalysts for the removal of water pollutants, Appl. Catal. B-Environ. 136 (2013) 9–18.
[9] J.A. Li, X.Y. Qiu, Y.Q. Lin, X.D. Liu, R.L. Gao, A.R. Wang, A study of modified Fe_3O_4 nanoparticles for the synthesis of ionic ferrofluids, Appl. Surf. Sci. 256 (2010) 6977–6981.
[10] L. Zhang, Z. Huang, H. Shao, Y. Li, H. Zheng, Effects of γ-Fe_2O_3 on γ-Fe_2O_3/Fe_3O_4 composite magnetic fluid by low-temperature low-vacuum oxidation method, Mater. Des. 105 (2016) 234–239.
[11] J.A. Gomes, G.M. Azevedo, J. Depeyrot, J. Mestnik, G.J. da Silva, F.A. Tourinho, R. Perzynski, $ZnFe_2O_4$ nanoparticles for ferrofluids: a combined XANES and XRD study, J. Magn. Magn. Mater. 323 (2011) 1203–1206.
[12] G.V.M. Jacintho, A.G. Brolo, P. Corio, P.A.Z. Suarez, J.C. Rubim, Structural investigation of MFe_2O_4 (M = Fe, Co) magnetic fluids, J. Phys. Chem. C 113 (2009) 7684–7691.
[13] C.C. Yang, X.F. Bian, J.Y. Qin, T.X. Guo, S.C. Zhao, Fabrication and hyperthermia effect of magnetic functional fluids based on amorphous particles, Appl. Surf. Sci. 330 (2015) 216–220.
[14] G. Stoian, H. Chiriac, Magnetic properties of CoFeSiB powders, suspensions, and in rigid matrix, IEEE Magn. 46 (2010) 495–497.
[15] M.C. Yu, C.C. Yang, X.F. Bian, S.C. Zhao, T.Q. Wang, S. Liu, T.X. Guo, Application of $Fe_{78}Si_9B_{13}$ amorphous particles in magnetorheological fluids, RSC Adv. 6 (2016) 22511–22518.
[16] Y. Pei, G.B. Zhou, N. Luan, B.N. Zong, M.H. Qiao, F. Tao, Synthesis and catalysis of chemically reduced metal-metalloid amorphous alloys, Chem. Soc. Rev. 41 (2012) 8140–8162.
[17] Y. Chen, Chemical preparation and characterization of metal-metalloid ultrafine amorphous alloy particles, Catal. Today 44 (1998) 3–16.
[18] H. Li, C.Z. Wang, Q.F. Zhao, H.X. Li, Co-B amorphous alloy nanochains with enhanced magnetization and electrochemical activity prepared in a biphasic system, Appl. Surf. Sci. 254 (2008) 7516–7521.
[19] P. Sarkar, O. Mohanta, S.K. Pal, A.K. Panda, A. Mitra, Magneto-impedance behavior of Co-Fe-Nb-Si-B-based ribbons, J. Magn. Magn. Mater. 322 (2010) 1026–1031.
[20] P. Sarkar, A.B. Mallick, R.K. Roy, A.K. Panda, A. Mitra, Structural and giant magneto-impedance properties of Cr-incorporated Co-Fe-Si-B amorphous microwires, J. Magn. Magn. Mater. 324 (2012) 1551–1556.
[21] X.Y. Yang, B. Yang, X.P. Li, Y. Cao, R.H. Yu, Structural-controlled chemical synthesis of nanosized amorphous Fe particles and their improved performances, J. Alloy Compd. 651 (2015) 551–556.
[22] M. Wen, M.F. Zhong, E. Kejia, J.D. Wu, L.J. Li, H.Q. Qi, S.X. Cao, T. Zhang, Soft magnetic Co-Fe-B-P and Co-Fe-V-B-P amorphous alloy nano-particles prepared by aqueous chemical reduction, J. Alloy Compd. 417 (2006) 245–249.
[23] A. Corrias, G. Ennas, G. Licheri, G. Marongiu, A. Mudinu, G. Paschina, G. Piccaluga, G. Pinna, Fe-Co-B amorphous alloy powder by chemical reduction, J. Mater. Sci. 7 (1988) 407–409.
[24] Z.Z. Yuan, D.P. Zhang, Preparation and magnetic properties of amorphous Co-Cu-B alloy nano-powders, Intermetallics 17 (2009) 281–284.
[25] A.L. Oppegard, F.J. Darnell, H.C. Miller, Magnetic properties of single-domain iron and iron-cobalt particles prepared by borohydride reduction, J. Appl. Phys. 32 (1961) S184.
[26] L. Yiping, G.C. Hadjipanayis, C.M. Sorensen, Magnetic and structural properties of ultrafine Co-B particles, J. Magn. Mater. 79 (1989) 321–326.
[27] J. Saida, A. Inoue, T. Masumoto, The effect of reaction condition on composition and properties of ultrafine amorphous powders in (Fe, Co Ni)-b systems prepared by chemical reduction, Metall. Trans. A 22 (1991) 2125–2132.
[28] D.D. Ke, Y. Tao, Y. Li, X. Zhao, L. Zhang, J.D. Wang, S.M. Han, Kinetics study on hydrolytic dehydrogenation of alkaline sodium borohydride catalyzed by Mo-modified Co-B nanoparticles, Int. J. Hydrogen Energy 40 (2015) 7308–7317.
[29] A. Zhukov, M. Churyukanova, S. Kaloshkin, V. Sudarchikova, S. Gudoshnikov, M. Ipatov, A. Talaat, J.M. Blanco, V. Zhukova, Magnetostriction of Co-Fe-based amorphous soft magnetic microwires, J. Electron. Mater. 45 (2016) 226–234.
[30] K. Gandha, K. Elkins, N. Poudyal, J.P. Liu, Synthesis and characterization of $CoFe_2O_4$ nanoparticles with high coercivity, J. Appl. Phys. 117 (2015) 17A736.
[31] A.O. Ivanov, S.S. Kantorovich, E.N. Reznikov, C. Holm, A.F. Pshenichnikov, A.V. Lebedev, A. Chremos, P.J. Camp, Magnetic properties of polydisperse ferrofluids: a critical comparison between experiment, theory, and computer simulation, Phys. Rev. E Stat. Nonlin. Soft Matter Phys. 75 (2007) 061405.
[32] P.J. Camp, E.A. Elfimova, A.O. Ivanov, The effects of polydispersity on the initial susceptibilities of ferrofluids, J. Phys. Condens. Matter 26 (2014) 456002.
[33] M.I. Shliomis, Magnetic fluids, Sov. Phys. Usp. 17 (1974) 153–169.
[34] V.S. Mendelev, A.O. Ivanov, Ferrofluid aggregation in chains under the influence of a magnetic field, Phys. Rev. E Stat. Nonlin. Soft Matter Phys. 70 (2004) 051502.
[35] A.O. Ivanov, V.S. Zverev, S.S. Kantorovich, Revealing the signature of dipolar interactions in dynamic spectra of polydisperse magnetic nanoparticles, Soft Matter 12 (2016) 3507–3513.
[36] A.O. Ivanov, Z. Wang, C. Holm, Applying the chain formation model to magnetic properties of aggregated ferrofluids, Phys. Rev. E Stat. Nonlin. Soft Matter Phys. 69 (2004) 031206.
[37] P. Debye, Einige resultate einer kinetischen theorie der isolatoren, Phisik. Zeits 13 (1912) 97–100.
[38] K.I. Morozov, A.V. Lebedev, The effect of magneto-dipole interactions on the magnetization curves of ferrocolloids, J. Magn. Magn. Mater. 85 (1990) 51–53.
[39] A.O. Ivanov, O.B. Kuznetsova, Magnetic properties of dense ferrofluids: an influence of interparticle correlations, Phys. Rev. E Stat. Nonlin. Soft Matter Phys. 64 (2001) 041405.
[40] S. Genc, B. Derin, Synthesis and rheology of ferrofluids: a review, Curr. Opin. Chem. Eng. 3 (2014) 118–124.
[41] M. Ashtiani, S.H. Hashemabadi, A. Ghaffari, A review on the magnetorheological fluid preparation and stabilization, J. Magn. Magn. Mater. 374 (2015) 716–730.
[42] K. Pandey, A.K. Shahi, R. Gopal, Magnetic colloid by PLA: Optical, magnetic and thermal transport properties, Appl. Surf. Sci. 347 (2015) 461–470.
[43] H.J. Chen, Y.M. Wang, J.M. Qu, R.Y. Hong, H.Z. Li, Preparation and characterization of silicon oil based ferrofluid, Appl. Surf. Sci. 257 (2011) 10802–10807.
[44] M. Klokkenburg, B.H. Erne, V. Mendelev, A.O. Ivanov, Magnetization behavior of ferrofluids with cryogenically imaged dipolar chains, J. Phys. Condens. Matter 20 (2008) 204113.